Peptide-Ruthenium Conjugate as an Efficient Photosensitizer for the Inactivation of Multidrug

Resistant Bacteria

Scott Pierce, Murphy P. Jennings, Samuel A. Juliano, and Alfredo M. Angeles-Boza *1,2

 Department of Chemistry, University of Connecticut, 55 N. Eagleville Road, Storrs, CT 06269, United States.

2. Institute of Materials Science, University of Connecticut, 97 N. Eagleville Road, Storrs, CT 06269, United States.

*E-mail: alfredo.angeles-boza@uconn.edu

Abstract

Antimicrobial photodynamic therapy (APDT) has gained increased attention due to its broad spectrum activity and lower likelihood to elicit bacterial resistance. Although many photosensitizers excel at eradicating gram-positive bacterial infections, they are generally less potent when utilized against gram-negative bacteria. We hypothesized that conjugating the DNA targeting, antimicrobial peptide, buforin II to a metal-based photosensitizer would result in a potent APDT agent. Herein, we present the synthesis and characterization of a buforin II-[Ru(bpy)₃]²⁺ (1) bioconjugate. The submicromolar activity of 1 against the multidrug resistant strains *Escherichia coli* AR 0114 and *Acinetobacter baumannii* Naval-17 indicates strong synergy between the ruthenium complex and buforin II. Our mechanistic studies point to an increased rate of DNA damage by 1, compared to [Ru(bpy)₃]²⁺. These results suggest that conjugating metal complexes to antimicrobial peptides can lead to potent antimicrobial agents.

Introduction

Antibiotic resistance is a quickly growing worldwide threat. Each year in the United States alone, 2.8 million people are infected with antibiotic resistant pathogens and 38,000 deaths result.¹ Although the long-term impact of antibiotic resistance remains uncertain,² there is agreement in that new antibiotics have to be brought into treatment.¹ Single target antibiotics such as β-lactams and quinolones have quickly elicited resistance in bacteria. These traditional antibiotics often target a single biological molecule or enzyme within a pathogen. Resistance can be easily achieved through mutations to target binding sites, production of enzymes to degrade the antibiotic, or upregulation of efflux pumps. However antibiotics and treatments that have less stringent targets such as daptomycin and antimicrobial photodynamic therapies (APDT), have demonstrated a lower occurrence of antimicrobial resistance development.^{3–5}

Photodynamic therapy typically requires three components, a photosensitizer, light, and molecular oxygen. Fradiation of the photosensitizer leads to the formation of reactive oxygen species (ROS) and the subsequent damage to cellular components leads to cell death. APDT have distinct advantages over traditional antibiotics as it is site specific, only when activated by light do photosensitizers elicit damage. This allows for targeted activity by only irradiating the infected region and minimizes off target effects which are commonly seen in traditional antibiotics. This targeted activity along with its low propensity to develop bacterial resistance has made APDT a promising avenue in medicine and approved therapies are being utilized in dentistry and dermatology. Many metal complexes are being investigated as photosensitizers for therapies other than APDT, APDT, although modifications would be necessary to produce ideal compounds for antimicrobial therapies. A common challenge is that many metal complexes possess poor ability

to cross cellular membranes, particularly those of gram-negative bacteria, due to their double membrane.^{17–19}

Antimicrobial peptides (AMPs) are one of the most promising molecular scaffolds being explored for the generation of much needed novel anti-infective agents. ^{20–23} AMPs possess several advantages as antimicrobial agents, such as broad spectrum activity and multiple-hit strategies.²⁴ ²⁷ But AMPs are not devoid of drawbacks as they often have low in vivo stability and low efficacy.²⁸ The latter is hypothesized to originate from the fact that AMPs evolved to defend a microenvironment after deployment of a relatively high concentration of a cocktail of peptides by the immune system.²⁹ Buforin II (TRSSRAGLOFPVGRVHRLLRK-NH₂) is a well-studied AMP that is notable for its broad spectrum antimicrobial activity, internal DNA target, and ability to facilitate the translocation of covalently linked molecules across the bacterial cell membrane. 30,31,32-34 Unfortunately, the peptide has not progressed to clinical trials, as it is not as potent as antibiotics used in the clinic. A truncated version of buforin II missing the N terminal TRSS amino acids has been shown to retain broad spectrum antimicrobial activity. Since previous studies have shown that the N terminus is not needed for antimicrobial activity, and that cargo covalently linked to the N terminus can be transported across membranes it presents an attractive location for modification.³⁵

As a proof-of-concept, we proceeded to couple $[Ru(bpy)_3]^{2+}$ to buforin II to overcome the difficulty of the former to cross bacterial cell membranes, and to capitalize on the oxidizing ability of singlet oxygen generated from photoactivated $[Ru(bpy)_3]^{2+}$. The N terminus of the peptide was chosen for conjugation since, as mentioned above, conjugation to the N terminus does not affect its membrane crossing activity.³³ We hypothesize that the antimicrobial activity of the

covalently linked [Ru(bpy)₃]²⁺—buforin II conjugate (1) would increase upon exposure to visible light in a synergistic fashion.

Scheme 1. Synthetic route for the [Ru(bpy)₃]²⁺—buforin II conjugate (1).

The monocarboxylic acid derivative of [Ru(bpy)₃]²⁺ (**RuBP-COOH**) used to synthesize **1** was prepared using previously reported methods.^{36,37} Synthesis of the C terminal amidated buforin II was completed on rink amide resin using standard Fmoc solid phase peptide synthesis protocols.³⁸ **RuBP-COOH** was then converted to an acyl chloride and allowed to react with the side chain protected buforin II on resin for 48 h (Scheme 1). **1** was then cleaved and purified to >95% via reversed phase HPLC and characterized using high resolution ESI TOF mass spectrometry.

To determine the effectiveness of **1** in comparison to unmodified buforin II we used a standard 96 well broth microdilution assay to determine minimum inhibitory concentration (MIC) against *Escherichia coli* and *Bacillus subtilis*, gram-negative and gram-positive bacteria, respectively.³⁹ Polypropylene 96-well plates were used to avoid binding of the peptide to the plate.^{21,39} Without irradiation, both buforin II and **1** showed the same MIC against *E. coli*, whereas the conjugate was 4-fold more active than the peptide when tested against *B. subtilis*. This result indicates that the addition of the metal complex to the N terminus of the peptide has only a minor effect on the antimicrobial efficacy of buforin II. Without irradiation, [Ru(bpy)₃]Cl₂ shows no

antimicrobial activity up to 64 μ M. When the same assay was repeated with 470 nm light irradiation (average intensity 12 mW/cm²), **1** showed a 32-fold and 16-fold decrease in its MIC against the gram-negative and gram-positive bacteria, respectively. Under irradiation, buforin II showed no increase in activity against *E. coli*, and just a two-fold change when tested against *B. subtilis*. The 1:1 mixture of [Ru(bpy)₃]Cl₂ and buforin II showed only a two-fold increase in activity under irradiation demonstrating that a covalent linkage is necessary for the synergistic interaction. 2-fold differences in MIC values can also be part of the error expected in this assay.³⁹

Table 1. Minimum inhibitory concentration (MIC) values determined for **1** and control compounds. Values are the mode of triplicate determinations and MICs are reported in μ M. Irradiation conditions: 470 nm light over 12 h (12mW/cm²)

	E. coli ((MG 1655)	B. subtilis (1A1)		
Compound	Dark	Irradiated	Dark	Irradiated	
Buforin II	32	32	16	8	
1	32	1	4	0.5	
Ru(bpy) ₃ Cl ₂	>64	>64	>64	>64	
Ru(bpy) ₃ Cl ₂ :1	32	16	16	8	

Previous studies have shown that buforin II binds to DNA after it enters the cytoplasmic space 34, thus, we hypothesized that the conjugate 1 is also able to internalize into the cytoplasmic space of the bacteria. To test this hypothesis, we incubated *E. coli* MG1655 with 1 and examined the cells using confocal fluorescence microscopy. The intrinsic fluorescence of the conjugate was monitored at an excitation of 457 nm and emission at 595 nm. 1 can be seen to enter the cells within 30 minutes (Figure 1, and z stack video available in SI). Ru polypyridyl complexes can cross membranes depending on their lipophilicity. However, [Ru(bpy)₃]Cl₂, at 8 μM, cannot cross the *E. coli* cell membrane within 30 minutes. Importantly, the microscopy results hint at the possibility of an internal target for 1.

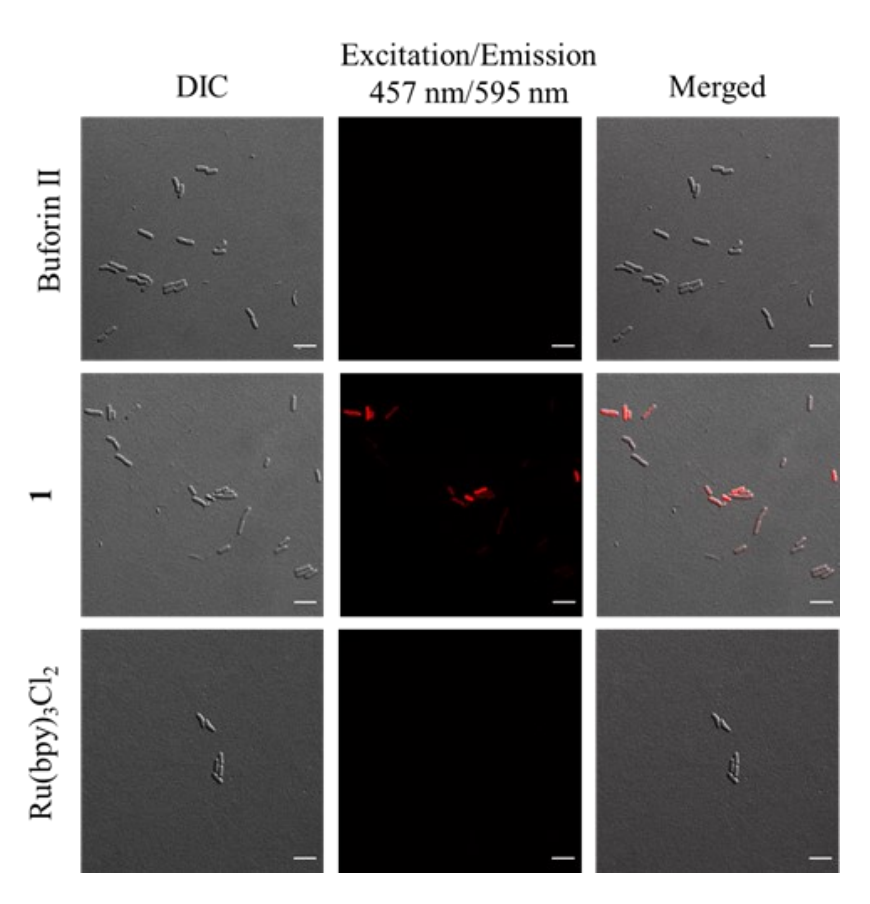


Figure 1. Laser confocal microscopy images of *E. coli* (MG 1655) exposed to 1 (8 μ M) for 30 minutes. Scale bars represent 5 μ m.

The internalization of **1** combined with the high DNA affinity of buforin II lead us to hypothesize that the increased activity of the ruthenium peptide conjugate was related to its ability to damage DNA.³⁰ To probe this idea, **1** was incubated with the plasmid pUC19 and irradiated (λ = 470 nm, 12mW/cm²) for up to 2 hours. Nicked DNA, which runs slower on an agarose gel, was detected, quantified, and compared to the supercoiled form (Figures 2A and S9).

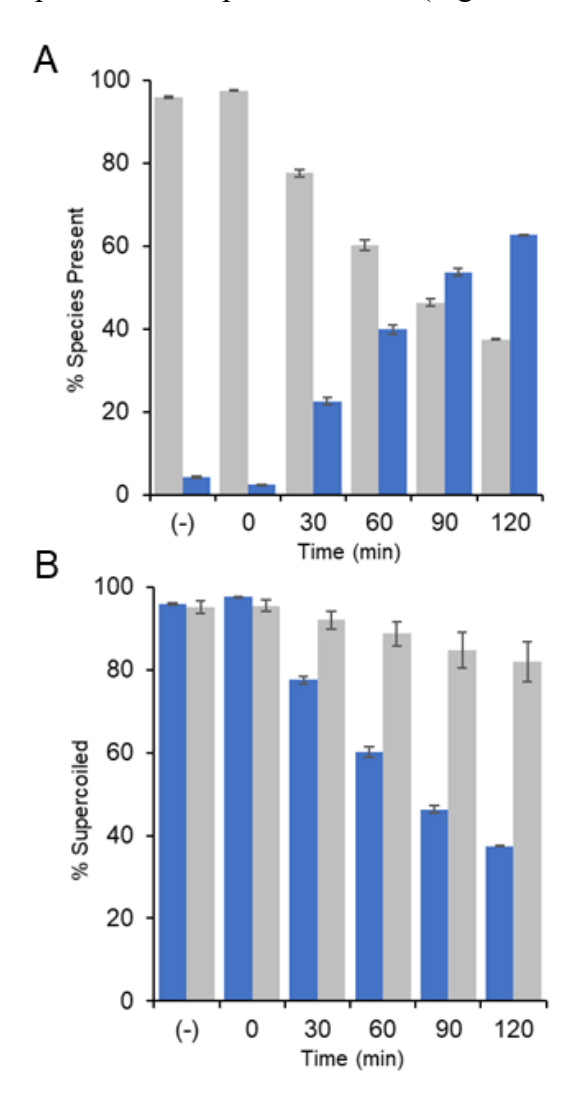


Figure 2. (A) Percentage supercoiled (\blacksquare) and nicked plasmid (\blacksquare) when pUC19 was incubated with 1 for 2 h. (B) Amount of supercoiled remaining when 20 μ M pUC19 was incubated with 1 (\blacksquare) and 1 and 10mM NaN₃ (\blacksquare) for 2 h.

As the irradiation time increased, the percentage of supercoiled DNA decreased and a subsequent rise in the nicked form was observed. The DNA damage seen is consistent with the increased antimicrobial activity of 1 when compared to buforin II under light irradiation. No DNA damage occurs without irradiation (Figure S9), consistent with the similar MICs determined for buforin II and 1 without light (Table 1). Nicked form is indicative of a single phosphodiester bond cleavage occurring and is consistent with results seen with other ruthenium complexes. When comparing the DNA photocleavage activity of 1 to that of unmodified [Ru(bpy)₃]²⁺ (Figure S12) it is evident that the degradation of the plasmid is approximately twice as great for 1. We attribute this increased rate of DNA damage by 1 to the large DNA binding affinity of buforin II. Binding of 1 to DNA via buforin II would allow for the photosensitizer to be in close proximity to the DNA and explains the increased rate of DNA degradation. Previous studies have shown that buforin II binds DNA, although it does not cleave DNA on its own. Our data suggests that the increased photo-induced antimicrobial activity of 1 is a consequence of bacterial DNA damage.

Two types of ROS are frequently cited for the activity observed for metal complex photosensitizers. Type 1 photosensitizers generate superoxide (O2*), hydroperoxyl (HO2*), and/or hydroxyl radicals (HO*), whereas Type 2 produce singlet oxygen ($^{1}O_{2}$). [Ru(bpy)3] $^{2+}$ derivatives are known to generate $^{1}O_{2}$ when irradiated in their metal to ligand charge transfer (MLCT) absorption band, placing them in the Type 2 group. The Diminished photocleavage would be expected when azide is added to the reaction mixture if $^{1}O_{2}$ were involved in the reaction of 1. Samples subjected to 10 mM NaN3 resulted in less photocleavage than those performed in its absence (Figure 2B). Repeating the experiment with scavengers for O_{2} , HO2*, and HO* showed minimal or no change when compared to those performed in their absence (Figures S13-S15). These results indicate that the formation of $^{1}O_{2}$ primarily drives the DNA cleavage. Stability

experiments show that under ambient light 1, roughly 35% of the conjugate is degraded. Faster degradation is observed when the sample is irradiated (470 nm, 12mW/cm², Figure S16). Since the conjugate is internalized within 30 minutes (*vide supra*), we believe 1 is the primary driver of cell death.

The mechanism of action demonstrated by 1 is suitable for broad spectrum activity, we determined its antimicrobial activity against the multidrug resistant (MDR) clinical isolates *Pseudomonas aeruginosa* AR 0229 (resistance; cephalosporin, and quinolones) *E. coli* AR 0114 (resistance; carbapenems and quinolones), *Acinetobacter baumannii* Naval-17 (multidrug resistant), and *Klebsiella pneumoniae* AR 0113 (resistance; β-lactams and aminoglycosides). The results clearly indicate that this approach is effective against pathogens that are clinically relevant (Table 2). Two interesting observations that deserve further studies are 1) the large increase in activity that occurs against *P. aeruginosa* AR 0229 (≥32-fold) and *K. pneumoniae* AR 0113 (16-fold); 2) without irradiation, 1 is more active than buforin II against *E. coli* AR 0114 and *A. baumannii* Naval-17. Studying antimicrobial mechanism of action and uncovering reasons behind the differences in activities against the different pathogens will provide important information on the structural aspects of peptide-metal complex conjugates that control their antimicrobial activity.

Table 2. MIC values determined for 1 and buforin II against antibiotic resistant clinical isolates, all MICs are reported in μ M. Irradiation conditions: 470 nm light over 12 h (12mW/cm²)

Compound	P. aeruginosa		E. coli		A. baumannii		K. pneumoniae	
	(AR 0229)		(AR 0114)		(Naval-17)		(AR 0113)	
	Dark	Irradiated	Dark	Irradiated	Dark	Irradiated	Dark	Irradiated
1	>64	2	4	0.5	4	0.5	64	4
Buforin II	>64	>64	16	16	16	16	64	64

In sum, our studies indicate strong synergy between the ruthenium complex and buforin II.

The peptide acts as a delivery agent to DNA allowing for localized production of ¹O₂ by the

ruthenium species, resulting in a more active bactericidal agent. This demonstrates that AMPs can

be made more efficient by conjugating them to metal complexes such as Ru(bpy)₃²⁺, increasing

the versatility of these chemical entities, and possibly leading to an increase of AMP drug

candidates. In particular, the submicromolar activity of 1 against the MDR strains E. coli AR 0114

and A. Baumannii Naval-17 suggests that conjugates of this type have significant potential.

ASSOCIATED CONTENT

Supporting Information.

The following files are available free of charge.

Additional experimental details (PDF)

Video E coli treated by 1 (AVI)

AUTHOR INFORMATION

Corresponding Author

Alfredo M. Angeles-Boza - Department of Chemistry and Institute of Materials Science,

University of Connecticut, Storrs, CT 06269, United States.

Email: alfredo.angeles-boza@uconn.edu

Author Contributions

The manuscript was written through contributions of all authors. All authors have given approval

to the final version of the manuscript.

ACKNOWLEDGMENTS

11

This work was supported by grants from the National Science Foundation (MCB-1715494 and CHE-1652606). Special thanks to Andrew Reardon for the TOC graphic.

REFERENCES

- (1) About Antibiotic Resistance | Antibiotic/Antimicrobial Resistance | CDC https://www.cdc.gov/drugresistance/about.html (accessed Aug 5, 2020).
- de Kraker, M. E. A.; Stewardson, A. J.; Harbarth, S. Will 10 Million People Die a Year Due to Antimicrobial Resistance by 2050? *PLoS Med.* **2016**, *13* (11), 1–6. https://doi.org/10.1371/journal.pmed.1002184.
- (3) Lauro, F. M.; Pretto, P.; Covolo, L.; Jori, G.; Bertoloni, G. Photoinactivation of Bacterial Strains Involved in Periodontal Diseases Sensitized by Porphycene–Polylysine Conjugates. *Photochem. Photobiol. Sci.* **2002**, *1* (7), 468–470. https://doi.org/10.1039/b200977c.
- (4) Schastak, S.; Ziganshyna, S.; Gitter, B.; Wiedemann, P.; Claudepierre, T. Efficient Photodynamic Therapy against Gram-Positive and Gram-Negative Bacteria Using THPTS, a Cationic Photosensitizer Excited by Infrared Wavelength. *PLoS One* **2010**, *5* (7), 1–8. https://doi.org/10.1371/journal.pone.0011674.
- (5) Tran, T. T.; Munita, J. M.; Arias, C. A. Mechanisms of Drug Resistance: Daptomycin Resistance. *Ann. N. Y. Acad. Sci.* **2015**, *1354* (1), 32–53. https://doi.org/10.1111/nyas.12948.
- (6) Arora, K.; Herroon, M.; Al-Afyouni, M. H.; Toupin, N. P.; Rohrabaugh, T. N.; Loftus, L.
 M.; Podgorski, I.; Turro, C.; Kodanko, J. J. Catch and Release Photosensitizers: Combining

- Dual-Action Ruthenium Complexes with Protease Inactivation for Targeting Invasive Cancers. *J. Am. Chem. Soc.* **2018**, *140* (43), 14367–14380. https://doi.org/10.1021/jacs.8b08853.
- (7) Roque, J.; Barrett, P. C.; Cole, H. D.; Lifshits, L.; Shi, G.; Monro, S.; von Dohlen, D.; Kim, S.; Russo, N.; Deep, G.; Cameron, C. G.; alberto, marta erminia; McFarland, S. A. *Breaking the Barrier: An Osmium Photosensitizer with Unprecedented Hypoxic Phototoxicity for Real World Photodynamic Therapy*; 2020. https://doi.org/10.1039/d0sc03008b.
- (8) McKenzie, L. K.; Bryant, H. E.; Weinstein, J. A. Transition Metal Complexes as Photosensitisers in One- and Two-Photon Photodynamic Therapy. *Coord. Chem. Rev.* **2019**, 379, 2–29. https://doi.org/10.1016/j.ccr.2018.03.020.
- (9) Dolmans, E. J. G. J. Dennis, Fukumura Dai, J. K. R. Photodynamic Therapy for Cancer.

 Nat. Rev. Cancer 2003, 3 (5), 380–387. https://doi.org/10.1038/nrc1071.
- (10) Knight, D. J. W.; Girling, K. J. Gut Flora in Health and Disease [9]. *Lancet* 2003, 361 (9371), 1831. https://doi.org/10.1016/S0140-6736(03)13438-1.
- (11) Kalghatgi, S.; Spina, C. S.; Costello, J. C.; Liesa, M.; Morones-Ramirez, J. R.; Slomovic, S.; Molina, A.; Shirihai, O. S.; Collins, J. J. Bactericidal Antibiotics Induce Mitochondrial Dysfunction and Oxidative Damage in Mammalian Cells. *Sci. Transl. Med.* 2013, 5 (192). https://doi.org/10.1126/scitranslmed.3006055.
- (12) Leman, J. A.; Morton, C. A. Photodynamic Therapy: Applications in Dermatology. *Expert Opin. Biol. Ther.* **2002**, *2* (1), 45–53. https://doi.org/10.1517/14712598.2.1.45.
- (13) Gursoy, H.; Ozcakir-Tomruk, C.; Tanalp, J.; Yilmaz, S. Photodynamic Therapy in

- Dentistry: A Literature Review. *Clin. Oral Investig.* **2013**, *17* (4), 1113–1125. https://doi.org/10.1007/s00784-012-0845-7.
- (14) Karges, J.; Heinemann, F.; Jakubaszek, M.; Maschietto, F.; Subecz, C.; Dotou, M.; Vinck, R.; Blacque, O.; Tharaud, M.; Goud, B.; Viñuelas Zahĺnos, E.; Spingler, B.; Ciofini, I.; Gasser, G. Rationally Designed Long-Wavelength Absorbing Ru(II) Polypyridyl Complexes as Photosensitizers for Photodynamic Therapy. *J. Am. Chem. Soc.* 2020, 142 (14), 6578–6587. https://doi.org/10.1021/jacs.9b13620.
- (15) Pickens, R. N.; Neyhouse, B. J.; Reed, D. T.; Ashton, S. T.; White, J. K. Visible Light-Activated CO Release and 1O2 Photosensitizer Formation with Ru(II),Mn(I) Complexes.

 Inorg. Chem.** 2018, 57 (18), 11616–11625.

 https://doi.org/10.1021/acs.inorgchem.8b01759.
- (16) Chen, Q.; Ramu, V.; Aydar, Y.; Groenewoud, A.; Zhou, X.; Jager, M. J.; Cole, H.; Cameron, C. G.; Mcfarland, S. A.; Bonnet, S.; Snaar-jagalska, B. E. TLD1433 Photosensitizer Inhibits Conjunctival Melanoma Cells in Zebrafish Ectopic and Orthotopic Tumor Models. *Cancers (Basel)*. 2020, 12 (3), 587. https://doi.org/https://doi.org/10.3390/cancers12030587.
- (17) Puckett, C. A.; Barton, J. K. Fluorescein Redirects a Ruthenium-Octaarginine Conjugate to the Nucleus. *J. Am. Chem. Soc.* **2009**, *131* (25), 8738–8739. https://doi.org/10.1021/ja9025165.
- (18) Liu, Y.; Qin, R.; Zaat, S. A. J.; Breukink, E.; Heger, M. Antibacterial Photodynamic Therapy: Overview of a Promising Approach to Fight Antibiotic-Resistant Bacterial Infections. J. Clin. Transl. Res. 2015, 1 (3), 140–167. https://doi.org/10.18053/jctres.201503.002.

- (19) Bolhuis, A.; Hand, L.; Marshall, J. E.; Richards, A. D.; Rodger, A.; Aldrich-Wright, J. Antimicrobial Activity of Ruthenium-Based Intercalators. *Eur. J. Pharm. Sci.* **2011**, *42* (4), 313–317. https://doi.org/10.1016/j.ejps.2010.12.004.
- Magana, M.; Pushpanathan, M.; Santos, A. L.; Leanse, L.; Fernandez, M.; Ioannidis, A.;
 Giulianotti, M. A.; Apidianakis, Y.; Bradfute, S.; Ferguson, A. L.; Cherkasov, A.; Seleem,
 M. N.; Pinilla, C.; de la Fuente-Nunez, C.; Lazaridis, T.; Dai, T.; Houghten, R. A.; Hancock,
 R. E. W.; Tegos, G. P. The Value of Antimicrobial Peptides in the Age of Resistance. *Lancet Infect. Dis.* 2020, 3099 (20), 1–15. https://doi.org/10.1016/S1473-3099(20)30327-3.
- (21) Mercer, D. K.; Torres, M. D. T.; Duay, S. S.; Lovie, E.; Simpson, L.; von Köckritz-Blickwede, M.; de la Fuente-Nunez, C.; O'Neil, D. A.; Angeles-Boza, A. M. Antimicrobial Susceptibility Testing of Antimicrobial Peptides to Better Predict Efficacy. *Front. Cell. Infect. Microbiol.* 2020, 10 (July), 1–34. https://doi.org/10.3389/fcimb.2020.00326.
- Agbale, C. M.; Sarfo, J. K.; Galyuon, I. K.; Juliano, S. A.; Silva, G. G. O.; Buccini, D. F.;
 Cardoso, M. H.; Torres, M. D. T.; Angeles-Boza, A. M.; De La Fuente-Nunez, C.; Franco,
 O. L. Antimicrobial and Antibiofilm Activities of Helical Antimicrobial Peptide Sequences
 Incorporating Metal-Binding Motifs. *Biochemistry* 2019, 58 (36), 3802–3812.
 https://doi.org/10.1021/acs.biochem.9b00440.
- (23) Thamri, A.; Létourneau, M.; Djoboulian, A.; Chatenet, D.; Déziel, E.; Castonguay, A.; Perreault, J. Peptide Modification Results in the Formation of a Dimer with a 60-Fold Enhanced Antimicrobial Activity. *PLoS One* **2017**, *12* (3), 1–12. https://doi.org/10.1371/journal.pone.0173783.
- (24) Juliano, S. A.; Serafim, L. F.; Duay, S. S.; Heredia Chavez, M.; Sharma, G.; Rooney, M.;

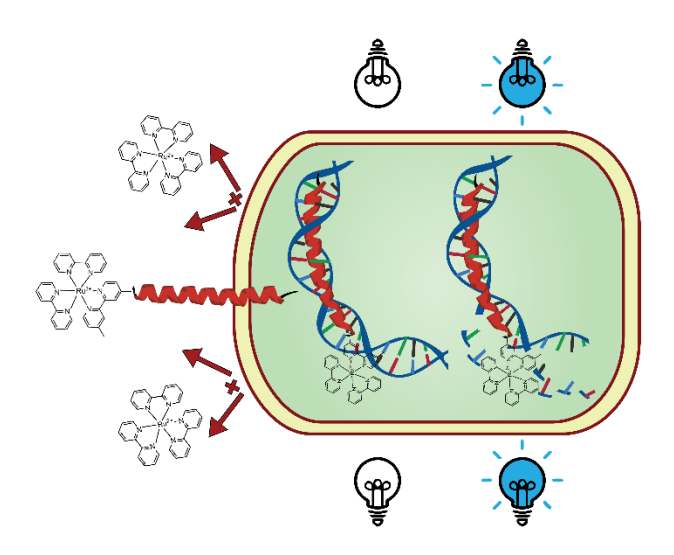
- Comert, F.; Pierce, S.; Radulescu, A.; Cotten, M. L.; Mihailescu, M.; May, E. R.; Greenwood, A. I.; Prabhakar, R.; Angeles-Boza, A. M. A Potent Host Defense Peptide Triggers DNA Damage and Is Active against Multidrug-Resistant Gram-Negative Pathogens. *ACS Infect. Dis.* **2020**, *6* (5), 1250–1263. https://doi.org/10.1021/acsinfecdis.0c00051.
- (25) Juliano, S. A.; Pierce, S.; Demayo, J. A.; Balunas, M. J.; Angeles-Boza, A. M. Exploration of the Innate Immune System of Styela Clava: Zn2+ Binding Enhances the Antimicrobial Activity of the Tunicate Peptide Clavanin A. *Biochemistry* **2017**, *56* (10), 1403–1414. https://doi.org/10.1021/acs.biochem.6b01046.
- Duay, S. S.; Sharma, G.; Prabhakar, R.; Angeles-Boza, A. M.; May, E. R. Molecular Dynamics Investigation into the Effect of Zinc(II) on the Structure and Membrane Interactions of the Antimicrobial Peptide Clavanin A. *J. Phys. Chem. B* **2019**, *123* (15), 3163–3176. https://doi.org/10.1021/acs.jpcb.8b11496.
- (27) Libardo, M. D. J.; Bahar, A. A.; Ma, B.; Fu, R.; McCormick, L. E.; Zhao, J.; McCallum, S. A.; Nussinov, R.; Ren, D.; Angeles-Boza, A. M.; Cotten, M. L. Nuclease Activity Gives an Edge to Host-Defense Peptide Piscidin 3 over Piscidin 1, Rendering It More Effective against Persisters and Biofilms. *FEBS J.* 2017, 284 (21), 3662–3683. https://doi.org/10.1111/febs.14263.
- (28) Koo, H. B.; Seo, J. Antimicrobial Peptides under Clinical Investigation. *Pept. Sci.* **2019**, 111 (5). https://doi.org/10.1002/pep2.24122.
- (29) Matsuzaki, K. Antimicrobial Peptides Basics for Clinical Apllication; Matsuzaki, K., Ed.; Springer Singapore, 2AD; pp 3–16. https://doi.org/10.1007/978-981-13-3588-4.

- (30) Uyterhoeven, E. T.; Butler, C. H.; Ko, D.; Elmore, D. E. Investigating the Nucleic Acid Interactions and Antimicrobial Mechanism of Buforin II. *FEBS Lett.* **2008**, *582* (12), 1715–1718. https://doi.org/10.1016/j.febslet.2008.04.036.
- (31) Xie, Y.; Fleming, E.; Chen, J. L.; Elmore, D. E. Effect of Proline Position on the Antimicrobial Mechanism of Buforin II. *Peptides* **2011**, *32* (4), 677–682. https://doi.org/10.1016/j.peptides.2011.01.010.
- (32) Takeshima, K.; Chikushi, A.; Lee, K. K.; Yonehara, S.; Matsuzaki, K. Translocation of Analogues of the Antimicrobial Peptides Magainin and Buforin across Human Cell Membranes. *J. Biol. Chem.* **2003**, *278* (2), 1310–1315. https://doi.org/10.1074/jbc.M208762200.
- (33) Libardo, M. D. J.; De La Fuente-Nuñez, C.; Anand, K.; Krishnamoorthy, G.; Kaiser, P.; Pringle, S. C.; Dietz, C.; Pierce, S.; Smith, M. B.; Barczak, A.; Kaufmann, S. H. E.; Singh, A.; Angeles-Boza, A. M. Phagosomal Copper-Promoted Oxidative Attack on Intracellular Mycobacterium Tuberculosis. *ACS Infect. Dis.* 2018, 4 (11), 1623–1634. https://doi.org/10.1021/acsinfecdis.8b00171.
- (34) Park, C. B.; Kim, H. S.; Kim, S. C. Mechanism of Action of the Antimicrobial Peptide Buforin II: Buforin II Kills Microorganisms by Penetrating the Cell Membrane and Inhibiting Cellular Functions. *Biochem. Biophys. Res. Commun.* **1998**, *244* (1), 253–257. https://doi.org/10.1006/bbrc.1998.8159.
- (35) Park, C. B.; Yi, K. S.; Matsuzaki, K.; Kim, M. S.; Kim, S. C. Structure-Activity Analysis of Buforin II, a Histone H2A-Derived Antimicrobial Peptide: The Proline Hinge Is Responsible for the Cell-Penetrating Ability of Buforin II. *Proc. Natl. Acad. Sci. U. S. A.*

- **2000**, 97 (15), 8245–8250. https://doi.org/10.1073/pnas.150518097.
- (36) Sullivan, B. P.; Salmon, D. J.; Meyer, T. J. Mixed Phosphine 2,2'-Bipyridine Complexes of Ruthenium. *Inorg. Chem.* **1978**, *17* (12), 3334–3341. https://doi.org/10.1021/ic50190a006.
- (37) Norrby, T.; Börje, A.; Åkermark, B.; Hammarström, L.; Alsins, J.; Lashgari, K.; Norrestam, R.; Mårtensson, J.; Stenhagen, G. Synthesis, Structure, and Photophysical Properties of Novel Ruthenium(II) Carboxypyridine Type Complexes. *Inorg. Chem.* 1997, 36 (25), 5850–5858. https://doi.org/10.1021/ic9705812.
- (38) Coin, I.; Beyermann, M.; Bienert, M. Solid-Phase Peptide Synthesis: From Standard Procedures to the Synthesis of Difficult Sequences. *Nat. Protoc.* **2007**, *2* (12), 3247–3256. https://doi.org/10.1038/nprot.2007.454.
- Wiegand, I.; Hilpert, K.; Hancock, R. E. W. Agar and Broth Dilution Methods to Determine the Minimal Inhibitory Concentration (MIC) of Antimicrobial Substances. *Nat. Protoc.* 2008, 3 (2), 163–175. https://doi.org/10.1038/nprot.2007.521.
- (40) Puckett, C. A.; Barton, J. K. Mechanism of Cellular Uptake of a Ruthenium Polypyridyl Complex. *Biochemistry* **2008**, *47* (45), 11711–11716. https://doi.org/10.1021/bi800856t.
- (41) Smithen, D. A.; Yin, H.; Beh, M. H. R.; Hetu, M.; Cameron, T. S.; McFarland, S. A.; Thompson, A. Synthesis and Photobiological Activity of Ru(II) Dyads Derived from Pyrrole-2-Carboxylate Thionoesters. *Inorg. Chem.* 2017, 56 (7), 4121–4132. https://doi.org/10.1021/acs.inorgchem.7b00072.
- (42) Baptista, M. S.; Cadet, J.; Di Mascio, P.; Ghogare, A. A.; Greer, A.; Hamblin, M. R.; Lorente, C.; Nunez, S. C.; Ribeiro, M. S.; Thomas, A. H.; Vignoni, M.; Yoshimura, T. M.

- Type I and Type II Photosensitized Oxidation Reactions: Guidelines and Mechanistic Pathways. *Photochem. Photobiol.* **2017**, *93* (4), 912–919. https://doi.org/10.1111/php.12716.
- (43) Angeles-Boza, A. M.; Bradley, P. M.; Fu, P. K. L.; Wicke, S. E.; Bacsa, J.; Dunbar, K. R.; Turro, C. DNA Binding and Photocleavage in Vitro by New Dirhodium(II) Dppz Complexes: Correlation to Cytotoxicity and Photocytotoxicity. *Inorg. Chem.* **2004**, *43* (26), 8510–8519. https://doi.org/10.1021/ic049091h.
- (44) Huang, H.; Yu, B.; Zhang, P.; Huang, J.; Chen, Y.; Gasser, G.; Ji, L.; Chao, H. Highly Charged Ruthenium(II) Polypyridyl Complexes as Lysosome-Localized Photosensitizers for Two-Photon Photodynamic Therapy. *Angew. Chemie Int. Ed.* **2015**, *54* (47), 14049–14052. https://doi.org/10.1002/anie.201507800.

FOR TOC ONLY



Synopsis

The conjugate Ru(bpy)₃-buforin II penetrates multidrug resistant gram-negative bacteria and causes cell death upon irradiation. This conjugate linearizes plasmid DNA and provides a new approach to combat antibiotic resistance.